

Comparing the Impact of Different Adsorbed Layers on the Local Glass Transition of Polymer Matrices

Michael F. Thees,¹ James H. Merrill,¹ Xinru Huang,¹ and Connie B. Roth^{1, a)}
Department of Physics, Emory University, Atlanta, Georgia 30322, USA

Submitted to the *Journal of Chemical Physics* for the special issue on “Polymer Nanoconfinement” on October 19, 2023, revised version submitted December 28, 2023

Chain adsorption to nanofiller interfaces creating bound layers has become central to understanding property changes in polymer nanocomposites. We determine the impact different kinds of adsorbed layers can have on the local glass transition temperature T_g of polymer matrices in a model film system using a localized fluorescence method. This work compares the adsorption and desorption of adsorbed layers grown in solution with the solution washing characteristics of adsorbed layers formed in the melt, leveraging knowledge about polymer adsorption in solution to infer the structure of adsorbed layers formed in the melt. In the limit of zero concentration after a long time in solution, we find that both kinds of adsorbed layers reach the same limiting adsorbed amount $h_\infty(c \rightarrow 0) \approx 1 \text{ nm}$, appearing to evolve to the same thermodynamic equilibrium state of a near monolayer of surface coverage. We propose that melt annealing leads to a coarsening of polymer segment–surface contacts, increasing the length of trains and shrinking loops and tails, slowing the subsequent kinetics of these adsorbed chains in solution. Considering how the pyrene-labeled chains intermix with the adsorbed layer enables us to discriminate between the impact of tails, loops, and trains, as threading of loops takes longer. We find that large fluffy loops, tails and trains have little to no impact on the local T_g . A large 30 K increase in local T_g is observed for 30-min solvent washed well-annealed films at long intermixing times that we attribute to the threading of small tight loops.

I. INTRODUCTION

Attachment of chains to interfaces is central to surface modification, adhesion, and reinforcement mechanisms in polymer materials.^{1–3} Explicitly grafted chains are used in some applications, but more common are surface bound chains that simply become adsorbed to the interface during processing.^{4–6} The degree of interpenetration between matrix chains and adsorbed chains will then be key to obtaining reinforcement in the polymer nanocomposite.^{7,8} Less appreciated is that the conformations of such adsorbed chains, and therefore their impact on the resulting material, will be different depending on how the material was formed.^{9–12} For example, a polymer nanocomposite cast from solution will end up with a “bound layer” where the adsorbed chains around the nanoparticles were formed in solution, compared to a polymer nanocomposite where the nanofiller and polymer were mixed by melt processing such that the “bound layer” was formed during melt annealing. This distinction typically goes unrecognized because the subsequent investigation and characterization of the surface adsorbed chains frequently employ solvent extraction to remove “unadsorbed chains” with the belief that the remaining polymer is representative of the bound layer in the melt.^{9,10,13,14}

In the present work, we compare chain adsorption in solution with solvent-washed melt-annealed films to investigate chain adsorption in the melt. Chain adsorp-

tion in solution is well understood having been heavily studied for decades dating back to the 1950s.¹⁵ Much of the understanding developed for uncharged polymer chains occurred from the 1970s-1990s culminating in the 1993 seminal book by Fleer, Cohen Stuart, Scheutjens, Cosgrove, and Vincent,¹ with additional key experiments demonstrating the motility of adsorbed chains in solution by Granick and coworkers.^{16–20} Even in the limit of strong adsorption (sticking energy $\chi_s \approx \text{several } kT$), adsorbed chain segments readily adsorb and desorb on the surface leading to highly mobile adsorbed chains that diffuse across the surface by crawling and even hopping.^{17,18} Thus, the long-standing notion of “irreversible adsorption” should be viewed as a dynamic equilibrium referring to the strong thermodynamic driving force based on the free energy of the entire system to maintain a given surface coverage in equilibrium with the bulk solution concentration.^{1,21}

Chain adsorption in melts has been comparatively little studied with most of it occurring during the past decade as the importance of nonequilibrium chain conformations near interfaces and the outsized impact of bound chains in nanocomposites have become recognized.^{4–6,22} The main issue limiting the investigation of chain adsorption in the melt is that the adsorbed chains next to the interface are intermixed with identical melt chains. The typical investigative procedure has been to use solvent as a means of exposing the adsorbed chains following a given thermal annealing treatment.^{9,14,23} This procedure, referred to as the “Guiselin experiment” or approach,⁹ relies on two theoretical assumptions made by Guiselin²⁴ that solvent washing removes only unadsorbed chains and exposes the “irreversibly adsorbed” chains unaltered

^{a)}To whom correspondence should be addressed:
 cbroth@emory.edu

from the melt state. However, these theoretical assumptions made by Guiselin in a computational analysis are experimentally unrealizable, having been demonstrated to be untrue.^{9,13} Yet use of the Guiselin procedure persists, having been employed to infer various structural features of adsorbed layers in the melt, including a two-stage adsorption process during thermal annealing in the melt above the glass transition temperature T_g .^{14,25-32} We recently reviewed this literature and tested the most commonly used procedure to create adsorbed layers from the melt by solvent washing melt-annealed films, concluding that the solvent washing strongly impacts the residual adsorbed layer thickness h_{ads} obtained after solvent washing.⁹

Here, we leverage the previous understanding developed about adsorbed chain behavior in solution to infer differences in chain adsorption that occur upon melt annealing near substrate interfaces, recognizing that once melt-annealed films are placed in solution to expose the adsorbed chains, the physics of the system must return to that known for polymer adsorption in solution resulting in mobile chains. We investigate the adsorption and desorption process of polymer chains in solution and melt systems, and determine the impact different kinds of adsorbed layers can have on the local glass transition temperature T_g of polymer matrices by using a localized fluorescence method. Focusing on a system with a polystyrene (PS) / silica interface that does not locally impact T_g by enthalpic interactions,³³⁻³⁶ we uncover the topological impact of adsorbed chains on T_g . Surface bound chains adsorbed and desorbed in solution are compared with the solution-washed melt-annealed films at different solvent washing stages to infer the most likely structure of adsorbed chains formed in the melt, as well as discriminate between the impact of loops, tails, and trains. Preformed adsorbed layers via different methods are intermixed with thin pyrene-labeled PS probe layers and then capped with a large PS matrix to enable the local glass transition temperature $T_g(z=0)$ next to the silica interface to be determined. Studying the impact of the intermixing time of the pyrene-labeled chains with the adsorbed layer is found to be key in deciphering the adsorbed layer's impact on local T_g as threading of loops takes longer than the intermixing of tails. We find that large fluffy loops, tails, and trains have little to no impact on $T_g(z=0)$, while it appears that the threading of small tight loops that we propose can form during prolonged thermal annealing in the melt state can strongly increase $T_g(z=0)$ by 30 K.

II. EXPERIMENTAL METHODS

Adsorbed layers of polystyrene (PS) with $M_w = 400$ kg/mol, $M_w/M_n = 1.06$ (Pressure Chemical), were made on silicon or quartz substrates by either immersing the substrates into a solution of PS in toluene of a given concentration c or by solvent washing spin-coated PS

films with toluene. All substrates were acid cleaned using hydrogen chloride (HCl) immediately prior to sample preparation by immersing the substrates into 10 vol% HCl for 30 min before being rinsed liberally and sonicated in DI water for 5 min, then dried with N_2 gas. We have previously demonstrated that this HCl acid cleaning method produces the same adsorbed layer thickness h_{ads} as the more commonly used piranha cleaning method of substrates.⁹ Both cleaning procedures remove organics and hydroxylate the surface, but the HCl acid cleaning method is less hazardous and logically easier.

Adsorbed layers grown from solution were done by placing the HCl cleaned substrates into toluene solutions with PS $M_w = 400$ kg/mol of different concentrations $c = 0.005$ mg/mL, 0.1 mg/mL, or 1.0 mg/mL for varying lengths of time. Adsorbed layers formed by solvent washing melt annealed films were made following the procedure that has become known as the "Guiselin experiment" or approach, reviewed in Ref. 9. Specifically, initial PS films of bulk thickness >200 nm were made by spin-coating a 2.5 wt% solution of PS $M_w = 400$ kg/mol in toluene at 800 rpm onto freshly cleaned substrates. For consistency, the same spin-coating conditions were always used, but the resulting $h_{ads}(t)$ values are independent of the initial film thickness for sufficiently thick films $>5-10R_g$,³¹ where for our 400 kg/mol M_w , 200 nm thick films are >10 times the radius of gyration R_g . Films were then annealed for 3 h, 6 h, or 23 h under vacuum at 150 °C, prior to being washed in toluene for a minimum of 30 min, or up to 30+ h, to form a residual adsorbed layer. During this procedure, samples were periodically removed from the solution and blown dry with N_2 gas to measure the current adsorbed layer thickness h_{ads} with ellipsometry, before being placed back into either the same solution or fresh solvent, both of which gave the same results. Similarly, adsorbed layers grown from $c = 1.0$ mg/mL solutions to reach the long-time plateau $h_\infty^{ads}(c)$, adsorbed amount $\Gamma_{ads}(c) = \rho h_\infty^{ads}(c)$, were also washed in pure toluene solvent, while having the h_{ads} thickness periodically measured. In this manner, the kinetics of desorption of the adsorbed layers in solution can be ascertained. Both types of adsorbed layers were washed in toluene solvent until a constant limiting $h_\infty(c \rightarrow 0)$ was reached, upwards of 100+ h in some cases.

Ellipsometry measurements to determine the thickness h_{ads} of the adsorbed layer on silicon substrates were done using spectroscopic ellipsometry (Woollam M-2000) at three angles of incidence, 55°, 60° and 65°, where the measured $\Psi(\lambda)$ and $\Delta(\lambda)$ data from all three angles were fit simultaneously for $\lambda = 400-1000$ nm. The optical layer model was comprised of three layers: a Cauchy layer $n(\lambda) = A + B/\lambda^2 + C/\lambda^4$ for the polymer layer with thickness h_{ads} , a native oxide layer, and a semi-infinite Si substrate.³⁷ The 1.32 nm thickness of the native oxide layer was determined from an average of multiple measurements across several different silicon wafers.⁹ Because the adsorbed layer is so thin, the refractive index $n(\lambda)$

of the PS adsorbed layer was held fixed at bulk PS parameter values $A = 1.563$, $B = 0.0079 \mu\text{m}^2$, and $C = 0.00038 \mu\text{m}^4$, determined from an average over multiple PS films of bulk thickness.^{9,37} This is commonly done when measuring the h_{ads} thickness of residual adsorbed layers^{9,23,28,31} because of the limitations that ellipsometry has to independently resolve film thickness and refractive index for very thin films less than $\approx 10 \text{ nm}$.^{38,39} For fluorescence measurements, the adsorbed layers need to be formed on quartz substrates. In these circumstances, identical adsorbed layers were formed simultaneously on quartz and silicon substrates, following the same procedure, by placing both substrates in the same solution. The thickness h_{ads} was then determined by measuring the adsorbed layer formed on the silicon. The silica surface chemistry of both quartz and silicon substrates with native oxide layers are the same such that we would expect the same adsorbed layer thickness h_{ads} to be formed on both.⁹

Fluorescence was used to determine the local glass transition temperature $T_g(z = 0)$ next to different adsorbed layers within bulk PS films by assembling samples with a multilayer geometry (see Fig. 3a) that intermixes a thin pyrene-labeled polystyrene (PS-Py) layer with the h_{ads} adsorbed layer prior to being capped by a thick, high molecular weight neat PS layer. Specifically, the sample preparation starts by forming an adsorbed layer of known thickness h_{ads} on quartz substrates following the procedures described above. A 12-nm thick PS-Py layer with 1.4 mol% pyrene content ($M_w = 672 \text{ kg/mol}$, $M_w/M_n = 1.3$) is then floated atop the h_{ads} layer using a water transfer method.^{34,36} This bilayer geometry is then annealed under vacuum at 170 °C for a time $t_{\text{mix}} = 2 \text{ h}$, 24 h, or 48 h to get the PS-Py chains to interpenetrate the adsorbed layer. A final 400 nm thick layer of neat PS ($M_w = 1,920 \text{ kg/mol}$, $M_w/M_n = 1.26$, Pressure Chemical) is then floated atop the bilayer. A final annealing step at 170 °C for 20 min is done of the entire multilayer sample to consolidate the layers into a single material with no air gaps. This sample preparation protocol creates films where the fluorescent PS-Py chains are intermixed with the surface bound chains at the substrate, enabling measurement of the local $T_g(z = 0)$ next to the adsorbed layer.^{34,36} As the total film thickness is $\approx 400 \text{ nm}$, the local $T_g(z = 0)$ next to the substrate interface is not affected by the free surface.

Fluorescence measurements were performed using a Photon Technology International QuantaMaster spectrophotofluorometer with samples mounted in an Instec HCS402 hot stage with MK1000 temperature controller. After equilibration of the sample at the starting temperature above T_g , the fluorescence intensity was monitored at a emission wavelength of 379 nm (6 nm band pass) on cooling at 1 °C/min, with excitation wavelength of 332 nm (4 nm band pass), following our previous works.^{34,36,40} After cooling, the sample was reheated to the starting temperature to ensure that the fluorescence intensity recovered was the same, verifying that no signif-

icant photobleaching occurred. Values of the glass transition temperature T_g were determined from the intersection of linear fits made to the liquid and glass lines of the temperature-dependent fluorescence intensity $I(T)$ above and below the transition. While individual $I(T)$ curves are shown in Figures 3 and 4, multiple measurements were collected on nominally identical samples to ensure reproducibility of the results. Bulk T_g for PS was determined from measurements on single layer films of 240 nm thickness with fluorescence giving a T_g^{bulk} of $99 \pm 3 \text{ °C}$, in agreement with the $T_g(z = 0) = 100 \pm 2 \text{ °C}$ measured for bare silica substrates with no adsorbed chains.³⁶

III. RESULTS AND DISCUSSION

A. Comparing Solvent Grown Adsorbed Layers and Solvent Washed Melt Annealed Films

1. Solvent Grown Adsorbed Layers

We start by characterizing the adsorption and desorption kinetics of polystyrene (PS) chains ($M_w = 400 \text{ kg/mol}$, $M_w/M_n = 1.06$) onto silica substrates in toluene at different concentrations. This well-understood behavior in solution will form our baseline for comparison. The choice of this relatively high molecular weight ensures that we will have substantial tails and loops of different sizes, and not merely flat trains as is common for low molecular weights.⁴¹ Freshly acid cleaned silicon substrates with native oxide layers SiOx–Si were immersed in toluene solutions with varying PS concentration. Such a PS/SiOx system in good solvent is considered weakly adsorbing with PS–silica “sticking” energies $\sim k_B T$ at room temperature.⁴³

In **Figure 1a**, we plot the adsorption kinetics as a function of time the SiOx–Si substrates spend in PS–toluene solutions of different concentrations: 1.0 mg/mL, 0.1 mg/mL, and $5 \times 10^{-3} \text{ mg/mL}$. The adsorbed amount $\Gamma = \rho h_{\text{ads}}$ is quantified by the adsorbed layer thickness $h_{\text{ads}}(t)$ measured by ellipsometry on dried samples periodically removed from solution,⁹ where Γ can be determined by multiplying h_{ads} with the density ρ of the dried polymer film. The dashed adsorption curves are fits of the $h_{\text{ads}}(t)$ data to a saturating exponential of the form

$$h_{\text{ads}}(t) = h_{\infty}^{\text{ads}}(c) \left[1 - e^{-t/\tau_{\text{ads}}} \right], \quad (1)$$

giving long-time adsorption plateau values $h_{\infty}^{\text{ads}}(c)$ of $5.1 \pm 0.2 \text{ nm}$ at 1 mg/mL and $0.9 \pm 0.2 \text{ nm}$ at 0.1 mg/mL. The time constant τ_{ads} was 0.8 h and 3.1 h for the 1 mg/mL and 0.1 mg/mL solutions, respectively, indicating that the adsorption process was slower at lower concentrations. At very low concentrations, the adsorption process is much slower, taking 96 hours to reach the long-time plateau of $h_{\infty}^{\text{ads}}(c) = 0.8 \pm 0.2 \text{ nm}$ for $c = 5 \times 10^{-3} \text{ mg/mL}$, because in extremely dilute solutions the kinetics for adsorption is diffusion limited¹ as the chains must

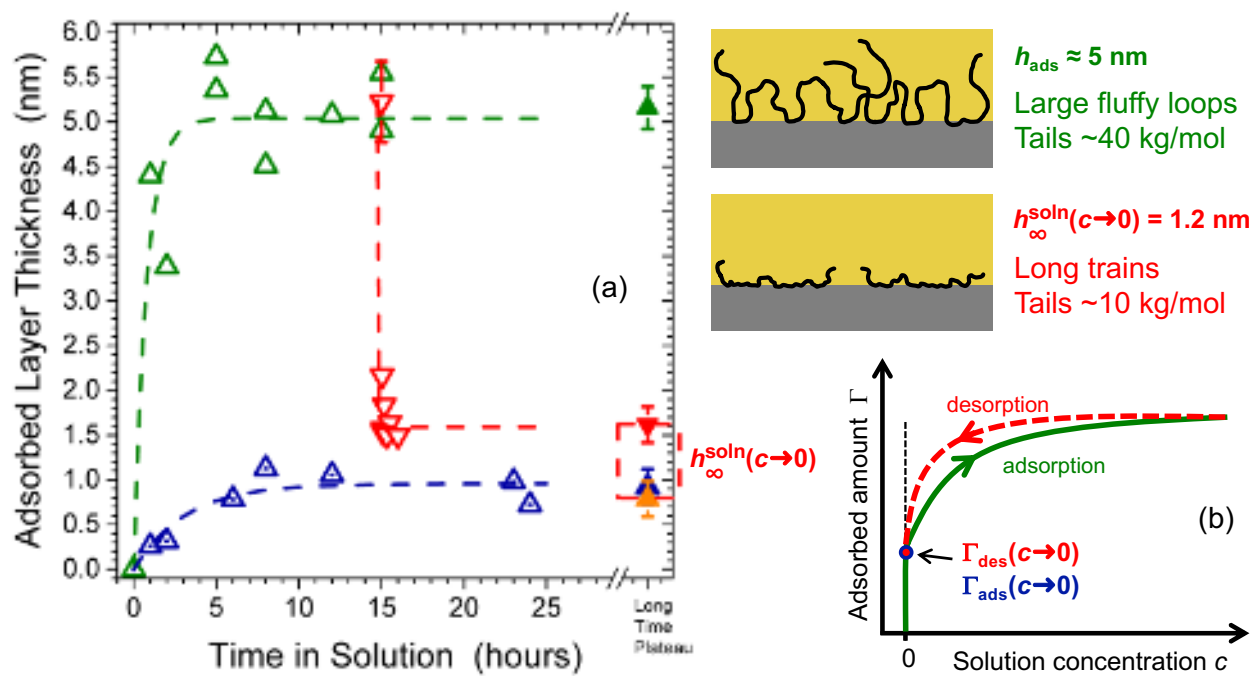


FIG. 1. (a) Measured adsorbed layer thickness $h_{\text{ads}}(t)$ as a function of time SiOx–Si substrates spend in toluene solution with PS chains ($M_w = 400 \text{ kg/mol}$) at different concentrations: $c = 1.0 \text{ mg/mL}$ (green upward pointing triangles), $c = 0.1 \text{ mg/mL}$ (blue dotted triangles), and $c = 5 \times 10^{-3} \text{ mg/mL}$ (orange solid triangle). Red downward pointing triangles show the desorption kinetics when $h_{\text{ads}} \approx 5 \text{ nm}$ adsorbed layers grown in solutions at $c = 1.0 \text{ mg/mL}$ are switched to pure toluene. Cartoon schematics are based on the Scheutjens and Fleer theory^{41,42} to estimate tail and loop lengths. (b) Schematic of adsorbed amount $\Gamma = \rho h_{\text{ads}}$ as a function of solution concentration c demonstrating hysteresis leading to the same limiting adsorbed amount in the limit of zero concentration on adsorption $\Gamma_{\text{ads}}(c \rightarrow 0)$ and desorption $\Gamma_{\text{des}}(c \rightarrow 0)$.

first find the substrate prior to adsorbing. However, the final adsorbed layer thickness $h_{\infty}^{\text{ads}}(c)$ reached at such low concentrations is to within experimental error the same as that reached at 0.1 mg/mL. Even at very low concentrations, the total free energy of the system favors having a near monolayer of surface coverage at the SiOx–Si substrate interface.^{1,21}

We have also characterized the desorption process by taking adsorbed layers with a long-time adsorption plateau value of $h_{\infty}^{\text{ads}}(c) = 5.1 \text{ nm}$ formed at $c = 1 \text{ mg/mL}$ and placing them in pure solvent. As shown in Fig. 1a, the kinetics of this desorption process for adsorbed layers grown in solution is very rapid, quickly reaching a limiting desorbed amount $h_{\infty}^{\text{des}}(c \rightarrow 0)$, where further time in solution or replacement with fresh pure solvent does not reduce this adsorbed amount further. These $h_{\text{ads}}(t)$ data were fit to an exponential decay of the form

$$h_{\text{ads}}(t) = \Delta h e^{-t/\tau_{\text{des}}} + h_{\infty}^{\text{des}}(c \rightarrow 0) \quad (2)$$

giving $\tau_{\text{des}} = 0.02 \text{ h}$ and $h_{\infty}^{\text{des}}(c \rightarrow 0) = 1.6 \pm 0.2 \text{ nm}$.

Interestingly, this limiting value of the adsorbed layer thickness on desorption $h_{\infty}^{\text{des}}(c \rightarrow 0)$ is within experimental error nearly the same as the long time plateau measured on adsorption at very low concentrations $h_{\infty}^{\text{ads}}(c \rightarrow 0)$. We highlight these long time limits at extremely low concentration by a dashed red box in Fig. 1a, identifying an average value of $h_{\infty}^{\text{soln}}(c \rightarrow 0) = 1.2 \pm 0.4 \text{ nm}$, which we

believe represents a near monolayer of surface coverage of chains for adsorbed layers formed in solution. This hysteresis in the adsorbed amount $\Gamma(c)$ on adsorption and desorption (increasing versus decreasing concentration), illustrated schematically in Fig. 1b, has been observed previously for polymer chains in solution.^{1,44,45}

2. Adsorbed Layers from Solvent Washed Melt Annealed Films

Most efforts to study chain adsorption in the melt take a spin-coated polymer film of bulk thickness and anneal it in its melt state for some prolonged length of time at a given temperature well above T_g .^{9,23,25,26,28} The resulting film is then washed with a good solvent, the details of which are highly variable and often vague,^{9,25,26,28} where the resulting solvent washed adsorbed layer is then used to comment on the state of the chains in the film near the substrate interface.^{14,25–32} However, in this process the resulting adsorbed layer in solvent is quite mobile and will restructure accordingly.^{16–19} When a polymer film is placed in pure solvent, solvent enters the film and chains diffuse away. This process continues until a solvent swollen adsorbed layer remains near the substrate surface. Initially the surface concentration of this adsorbed layer is extremely high such that unadsorbed chains with

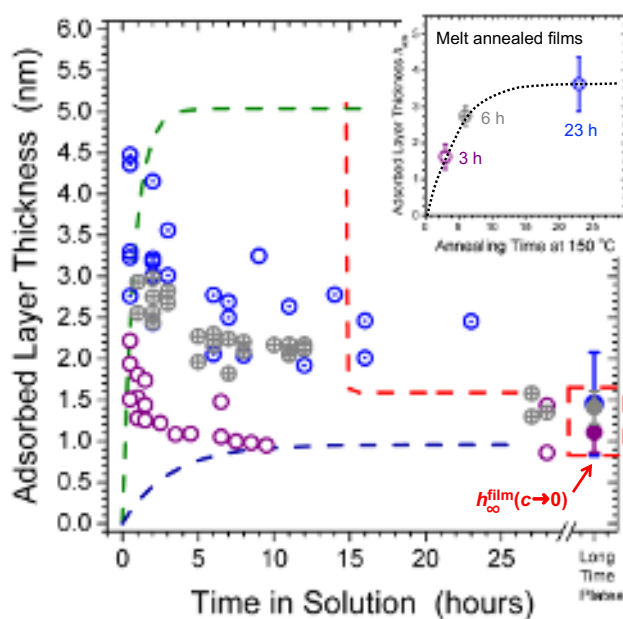


FIG. 2. Measured residual adsorbed layer thickness h_{ads} of polymer films melt annealed at 150 °C for 3 h (purple open circles), 6 h (gray crossed circles), and 23 h (blue dotted circles) as a function of solvent washing time in pure toluene. Adsorbed layers from melt annealed films show a continual decrease in h_{ads} until they reach a minimum limiting adsorbed layer thickness $h_{\infty}^{\text{film}}(c \rightarrow 0) = 1.3 \pm 0.6 \text{ nm}$, where the long time plateau values are shown as filled circles. For comparison, the dashed curves are the fits to the data in Fig. 1a showing the trends for the adsorbed layers in solution. Inset shows the average $h_{\text{ads}}(t)$ after 30 min of washing the films as a function of time annealing the film at 150 °C, typical of the procedure commonly used in the literature.

no direct substrate contacts may be pinned under loops of adsorbed chains. Even though this adsorbed layer may be far from an equilibrium adsorbed layer formed in solution, the same physics must apply to the system. Over time in solution, the adsorbed layer will slowly restructure with polymer segment–substrate contacts continuously desorbing and readsorbing on the surface allowing some chains to diffuse away. As more chains diffuse away, the remaining chains will slowly form an adsorbed layer that is similar to one formed on desorption in dilute solution. Based on experimental observations, Granick has suggested that large scale restructuring of an adsorbed layer in solution can take many hours.^{46,47}

We try to elucidate this process in **Figure 2** by taking spin-coated PS films ($M_w = 400 \text{ kg/mol}$, 200 nm thick) that were annealed in the melt state at 150 °C ($T_g + 50 \text{ K}$) for 3 h, 6 h, or 23 h, and then monitoring how their residual adsorbed layer thickness h_{ads} evolves with time in solution. The thickness of the adsorbed layer h_{ads} is measured in a dry state by periodically removing the sample from the toluene solution, drying it, and determining its thickness with ellipsometry.⁹ The concentration of this solution is extremely low, where immersing

the entire film already corresponds to a concentration of only $c \approx 10^{-3} \text{ g/mL}$ for a 200 nm thick film (laterally 2 cm \times 2 cm) dissolved in 100 mL of toluene. We observe that with prolonged time in solution, all the adsorbed layers evolve to the same limiting h_{ads} value of $h_{\infty}^{\text{film}}(c \rightarrow 0) = 1.3 \pm 0.6 \text{ nm}$, which we find to be equivalent to the limiting adsorbed layer formed in solution at extremely low concentrations $h_{\infty}^{\text{soln}}(c \rightarrow 0) = 1.2 \pm 0.4 \text{ nm}$. We note that this limiting h_{ads} value of $h_{\infty}^{\text{film}}(c \rightarrow 0)$ is comparable to limiting residual adsorbed layers found by Koga et al. termed “flattened layers” after extreme solvent washing of films over 120 days in toluene or several days in the more aggressive solvent chloroform.^{25–27}

3. Adsorbed Amount in the Limit of Zero Concentration

The adsorption process in solution is typically treated as a thermodynamic process where the total free energy of the system is minimized by having the fewest molecules in contact with the substrate interface because this causes the smallest reduction in the total entropy.^{1,21,41,42,48} As an individual polymer chain takes up more surface area than an individual solvent molecule, a layer of polymer chains will eventually coat the substrate interface. The observation in Fig. 1a that we reach the same limiting adsorbed amount $h_{\infty}^{\text{ads}}(c \rightarrow 0) \approx 1 \text{ nm}$ at long times for the two lowest concentrations $c = 0.1 \text{ mg/mL}$ and $c = 5 \times 10^{-3} \text{ mg/mL}$ strongly suggests that this is a thermodynamic equilibrium state likely corresponding to a near monolayer of surface coverage with few chains remaining in the bulk solution.

Interestingly, on desorption in solution, the same limiting adsorbed amount $h_{\infty}^{\text{des}}(c \rightarrow 0)$ is basically being reached in the limit of zero concentration, suggesting the system is evolving to the same thermodynamic equilibrium state corresponding to a near monolayer of surface coverage. This is in contrast to the interpretation put forward by Fleer et al. that the limiting desorbed amount $h_{\infty}^{\text{des}}(c \rightarrow 0)$ should be viewed as effectively a kinetically trapped nonequilibrium state²² where repeated exchanges with pure solvent represent such a small change in the bulk solution concentration that any further desorption of chains from the substrate needed to reestablish a new equilibrium solution concentration represent a tiny change in the adsorbed amount at the substrate interface.¹ Fleer et al. cautioned that the remaining adsorbed amount after repeated exchanges with pure solvent should not be viewed as an indication that the adsorbed layer is irreversibly adsorbed, but simply that further desorption becomes insignificantly small.¹ Given the results of Fig. 1a, it appears there is an equilibrium adsorbed amount $\Gamma_{\text{eq}}(c \rightarrow 0)$ in the limit of low concentration that the system is trying to maintain. However, we stress that all experimental evidence suggests this is a dynamic equilibrium²¹ where the adsorbed chains at the substrate interface are still exceedingly mobile and readily exchange with those in the bulk solution.^{16–19,49}

In Fig. 2, we find that adsorbed layers formed by solvent washing melt annealed films are also slowly reaching this same residual adsorbed amount $h_\infty^{\text{des}}(c \rightarrow 0)$ in the limit of zero concentration. Given the high mobility of adsorbed chains in solution,^{16–19,49} perhaps this evolution is unsurprising because the system is effectively the same, a layer of polymer chains at the substrate interface in thermodynamic equilibrium with a solution of extremely low concentration. Thus, the same physics must apply. These results then suggest that all the adsorbed layers at extremely low concentrations in the limit of spending a long time in solution $h_\infty(c \rightarrow 0)$ are equivalent, regardless of whether they were formed in solution or by solvent washing melt annealed films.

However, Fig. 2 also shows that films that were annealed for a longer amount of time in the melt state prior to being placed in solution take longer to reach this limiting plateau value in residual adsorbed layer thickness $h_\infty(c \rightarrow 0)$: ~ 5 h, ~ 25 h, and >100 h for the 3 h, 6 h, and 23 h of melt annealing, respectively. Thus, it is clear that some evolution of the chains near the substrate interface has occurred during melt annealing of the films, and that this has subsequently slowed their kinetics in solution. As we will discuss in section III C, we suspect that melting annealing causes a coarsening of polymer segment–surface contacts such that the length of trains increase for the chains that have the largest number of polymer segment–surface contacts making these chains remaining at the substrate interface harder to displace in solution.

B. Comparing Local T_g Next to Different Types of Adsorbed Layers

In terms of understanding polymer material properties near interfaces, we are most interested in characterizing how different adsorbed layers may impact the local dynamics of a neighboring polymer matrix. To do this, we use a localized fluorescence method to measure the local T_g of pyrene-labeled polymer chains intermixed with the different adsorbed layers. The multilayer sample geometry constructed for these measurements is depicted in **Figure 3a**. We start by forming the desired type of adsorbed layer as described in the previous section. A 12 nm thick pyrene-labeled PS probe layer with 1.4 mol% pyrene content ($M_w = 672$ kg/mol, $M_w/M_n = 1.3$)^{34,36,50,51} is then floated immediately atop the adsorbed layer, and these two layers are then intermixed by annealing this bilayer for a time t_{mix} at 170 °C. As we will demonstrate, this intermixing time t_{mix} is very important and informative for understanding how different parts of the adsorbed layer can alter the local T_g of a neighboring polymer matrix. After the dye-labeled probe layer has intermixed with the adsorbed layer, a bulk PS layer ($M_w = 1,920$ kg/mol, $M_w/M_n = 1.26$) is placed on top to cap the probe layer, creating samples where the local glass transition temperature $T_g(z = 0)$ next to this

adsorbed layer interface can be measured without any impact from free surface effects. Immediately prior to these localized T_g fluorescence measurements, the samples are further annealed at 170 °C for 20 min to ensure all the individual layers have formed a consolidated sample with no air gaps and to equilibrate the sample above T_g removing any thermal history. This is the same sample geometry that our group previously used to measure the local $T_g(z = 0)$ next to end-grafted chains.^{34,36} In these multilayer samples, high molecular weights are used for the layers to limit diffusion of the pyrene-labeled probe layer during the fluorescence measurement.^{34,36,50} We note our sample geometry is measuring the local T_g of the polymer chains intermixed with the adsorbed layer to identify the impact the adsorbed layer can have on the local matrix chains, as opposed to other studies that have measured the local T_g of the adsorbed layer.^{52–55}

For our measurements of the local $T_g(z = 0)$ next to silica interfaces with different adsorbed layers, we will make comparisons between two groups of adsorbed layers formed with the $M_w = 400$ kg/mol PS. Group 1 will compare relatively thick adsorbed layers with $h_{\text{ads}} \approx 4.5$ nm either formed in solution or by solvent washing melt annealed films. Specifically, the solution grown adsorbed layers were formed in a $c = 1$ mg/mL toluene solution giving a long-time plateau value of $h_{\text{ads}} = 5.2$ nm. The solvent washed films were formed by annealing bulk PS films for 23 h at 150 °C and then washing them in toluene for 30 min to give residual adsorbed layer thicknesses of $h_{\text{ads}} = 3.6$ nm. This procedure is typical of that commonly used in the literature to obtain residual adsorbed layers by solvent washing melt annealed films. Group 2 will compare adsorbed layers with $h_{\text{ads}} \approx 1$ nm formed after a long time in solution in the limit of extremely low concentration $h_\infty(c \rightarrow 0)$. This will include solution grown adsorbed layers formed at $c = 0.1$ mg/mL with $h_{\text{ads}} = 0.9$ nm, as well as films annealed at 150 °C for either 3 h or 23 h and then subsequently washed in solvent for 100+ hours to reach $h_{\text{ads}} = 1.4$ nm and 1.1 nm, respectively.

To measure the local glass transition temperature $T_g(z = 0)$ of the pyrene-labeled PS chains intermixed with the adsorbed layer, the fluorescence intensity $I(T)$ of pyrene is monitored at 379 nm, corresponding to the first peak of the pyrene emission spectrum that is highly sensitive to its local environment,^{56,57} on cooling the multilayer sample at 1 °C/min.^{34,36,40,50,51} The temperature dependence of the fluorescence intensity reflects the local density, polarity, and stiffness of the polymer matrix surrounding the dye, where the glass transition temperature T_g is identified by the intersection of linear fits to the liquid and glass regimes.^{33,34,36,40,50,51}

1. Group 1: 5 nm Adsorbed Layers

Figure 3b shows representative plots of the temperature dependent fluorescence intensity $I(T)$ for the two

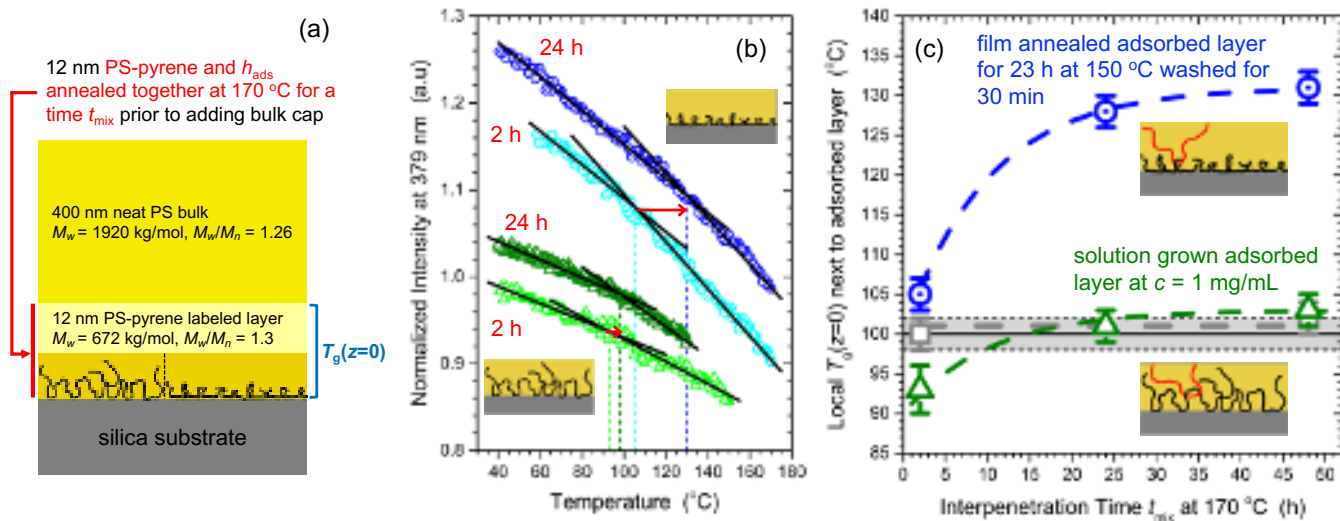


FIG. 3. (a) Schematic of the sample geometry used to measure the local T_g via fluorescence adjacent to the adsorbed layer. (b) Temperature dependent fluorescence intensity for pyrene-labeled PS probe layers adjacent to the $h_{\text{ads}} \approx 4.5 \text{ nm}$ adsorbed layers of Group 1, $c = 1.0 \text{ mg/mL}$ solution grown adsorbed layers (green triangles) and 30 min solvent-washed films annealed for 23 h at 150 °C (blue circles), where the lighter colors correspond to an intermixing time $t_{\text{mix}} = 2 \text{ h}$ and the darker colors are for $t_{\text{mix}} = 24 \text{ h}$. (c) Changes in local $T_g(z = 0)$ next to the adsorbed layers with increasing intermixing time t_{mix} at 170 °C used to interpenetrate the pyrene-labeled probe layer with the adsorbed layer prior to the local T_g measurement.

different types of adsorbed layers of Group 1, solution grown versus solvent washed films, with $h_{\text{ads}} \approx 4.5 \text{ nm}$. Data are shown for two different intermixing times $t_{\text{mix}} = 2 \text{ h}$ and 24 h for each type of adsorbed layer, demonstrating that this intermixing time t_{mix} at 170 °C can have a significant impact on the measured local $T_g(z = 0)$ value. For the $c = 1.0 \text{ mg/mL}$ solution grown adsorbed layer, the local $T_g(z = 0)$ next to the adsorbed layer increases from 93 °C for $t_{\text{mix}} = 2 \text{ h}$ to 98 °C for $t_{\text{mix}} = 24 \text{ h}$. The impact of increasing t_{mix} is more significant for the 30 min solvent washed films annealed for 23 h at 150 °C, where the local $T_g(z = 0)$ next to the adsorbed layer increases from 105 °C for $t_{\text{mix}} = 2 \text{ h}$ to 130 °C for $t_{\text{mix}} = 24 \text{ h}$. For comparison, equivalent measurements of the local $T_g(z = 0)$ next to bare silica substrates give $T_g = 100 \pm 2 \text{ °C}$, equivalent to bulk T_g .^{33–36} We note that even when the pyrene-labeled probe layer is annealed for up to 48 h at 170 °C on the bare silica substrate the local T_g value still reports bulk T_g .³⁶

Annealing at 170 °C for an intermixing time t_{mix} enables the pyrene-labeled PS matrix chains to interpenetrate with the adsorbed layer. From these results we can conclude that good intermixing between the adsorbed chains and the pyrene-labeled PS chains is necessary for local T_g increases to occur. This observation is consistent with previous work showing local T_g changes near polymer-polymer interfaces only when the interface was annealed to equilibrium.^{51,58} How long of an intermixing time t_{mix} is required is a somewhat unknown process. Adsorbed layers consist of three main structural elements: tails, loops, and trains. Intermixing between the pyrene-labeled PS chains and the adsorbed chains

will occur for tails and loops, while trains are simply monomers that lie flat along the substrate interface.

The interpenetration of tails with a high molecular weight polymer matrix presumably occurs in a manner similar to end-grafted polymer chains, which is a system that has been well studied.² Experimentally, the time scale and degree of interpenetration between end-tethered polymer chains and a high molecular weight polymer matrix has been measured using neutron reflectivity for different annealing conditions.^{59–61} Theoretically, interpenetration is understood as resulting from chain-end retraction “breathing” modes that extend the end-tethered chains into the matrix.^{62,63} It is based on these literature studies that our group’s previous works studying $T_g(z = 0)$ next to end-grafted chains selected 2 h at 170 °C as the annealing conditions necessary to ensure good interpenetration of end-grafted chains with the pyrene-labeled PS layer.^{34,36} For this reason, we use a minimum intermixing time $t_{\text{mix}} = 2 \text{ h}$, where we believe that at this stage tails of the adsorbed layer will be well intermixed with the pyrene-labeled PS matrix chains.

The intermixing with loops of the adsorbed layer by the pyrene-labeled PS matrix chains is more challenging and therefore expected to require a much longer intermixing time t_{mix} due to the additional topological constraints. Interpenetration with loops requires threading of the loops by the high molecular weight pyrene-labeled PS matrix chains. The dynamics of this process will be set by the reptation time of the pyrene-labeled PS chains ($M_w = 672 \text{ kg/mol}$), but the probability of threading will be strongly dependent on the size of the loops.⁶⁴ Small tight loops can be expected to take longer to thread than

larger fluffy loops. Given the unknown time scale needed for this process, we therefore explored the effect that increasing intermixing time t_{mix} has on the measured local T_g . **Figure 3c** plots the measured local $T_g(z = 0)$ next to the substrate interface with the given adsorbed layer as a function of increasing t_{mix} at 170 °C for both types of adsorbed layers from Group 1, solution grown and solvent washed films with $h_{\text{ads}} \approx 4.5$ nm. In both cases, the local $T_g(z = 0)$ is observed to increase and saturate for $t_{\text{mix}} > 24$ h at 170 °C, although be it at significantly different values. The values plotted in Fig. 3c are the average and standard deviation of multiple measurements on nominally identical samples. For the $c = 1.0$ mg/mL solution grown adsorbed layer with $h_{\text{ads}} = 5.2$ nm, $T_g(z = 0)$ is initially measured to be below T_g^{bulk} at only 93 ± 3 °C after 2 h of annealing at 170 °C, and then saturates to 103 ± 2 °C after 48 h of annealing. In contrast, the 30 min solvent washed films that had been annealed for 23 h at 150 °C giving $h_{\text{ads}} = 3.6$ nm, initially report a $T_g(z = 0) = 105 \pm 2$ °C after 2 h of annealing at 170 °C, and then saturates to $T_g(z = 0) = 131 \pm 2$ °C after 48 h. Figure 3c also shows measured $T_g(z = 0)$ values for the pyrene-labeled probe layer next to the bare silica substrate that were similarly annealed for up to 48 h at 170 °C, where $T_g(z = 0)$ remains at 100 ± 2 °C, equivalent bulk T_g for PS.

We believe that desorption of the 400 kg/mol adsorbed chains is not occurring during the annealing at 170 °C. Desorption has been experimentally observed at such elevated temperatures in polymer nanocomposites and films for adsorbed chains with molecular weights of ~ 100 kg/mol or less.^{11,65,66} However, there is a strong molecular weight dependence to desorption as the adsorbed chains must unzip from the substrate interface releasing all their adsorbed monomers before the desorbed chain can diffuse away.^{20,21,66} For example, Bailey et al. found for solution grown adsorbed layers that the desorption time scale increased by roughly a factor of 10 for an increase in molecular weight of only a factor of 3.⁶⁵ In addition, if we compare the desorption time scales from Bailey et al.⁶⁵ for solution grown adsorbed layers with that of Jimenez et al.¹¹ on adsorbed layers formed by melt annealing, it appears that the melt annealed adsorbed layers take roughly 4 times longer to desorb for equivalent molecular weights at comparable desorption temperatures. Ren et al. showed that the time scale for desorption increased exponentially with chain length N as $\exp(N^{1/2})$, where PS chains with molecular weights > 57 kg/mol where not observed to desorb even after 120 h of annealing at 170 °C for these adsorbed layers made by solvent washing well-annealed films.⁶⁶ Based on the time scales reported in these studies, we can conclude that desorption would take well in excess of the 48 h of annealing we performed at 170 °C. Figure 2 already demonstrated that the adsorbed chains from melt-annealed films are strongly adhered to the silica substrate interface as they require an extremely long time (100+ h) in solution to wash off and reduce the measured h_{ads}

value.

We are also able to safely rule out that the ≈ 30 K $T_g(z = 0)$ increase observed for the adsorbed layers from solvent-washed melt-annealed films is not due to adsorption of pyrene-labeled PS chains resulting from an exchange of adsorbed chains at the substrate interface. As shown in Fig. 3c, annealing of the pyrene-labeled PS probe layer directly next to the bare silica substrate did not result in any $T_g(z = 0)$ increase even after 48 h of annealing at 170 °C. This observation is consistent with there being no enthalpic drive for adsorption in a melt as there is no reason to favor one polymer segment–surface contact over another. This point is discussed further in section III C where the definition of the substrate sticking energy, Eq. (3), is considered.

A puzzling aspect about these results is that we find no evidence of local T_g increases when pyrene-labeled chains are annealed in the melt state next to bare silica substrates. In this and previous studies, we have explicitly tested pyrene-labeled probe layers annealed at temperatures of 120-130 °C and 170 °C for annealing times spanning from 30 min to upwards of 48 hours.³⁴⁻³⁶ These are similar to conditions under which others claim chain adsorption is occurring in the melt. Napolitano et al. has reported chain adsorption occurring when melt annealing PS films on silicon substrates with native oxide layers at temperatures between 140 and 180 °C for times spanning from 1 to 60 hours, based on residual adsorbed layer thicknesses h_{ads} obtained after solvent washing.²⁸ Koga et al. has reported the same residual adsorbed layer thickness h_{ads} obtained after five 10-min solvent washes in toluene for PS films annealed between 40 and 150 °C for 24 hours.²⁵ Under conditions similar to where others have claimed chain adsorption is occurring during melt annealing, we observe no local T_g increase with pyrene-labeled chains. Also noteworthy is that Priestley et al., who adsorbed pyrene-labeled chains to measure the local T_g of the adsorbed chains, have never reported a T_g higher than bulk.^{52,53} Thus, we find that simply annealing polymer chains near a substrate interface in a melt state at high temperature does not result in an increase in local T_g . In contrast, it appears to us that solvent washing the films is an essential step to forming adsorbed layers.⁹ The $T_g(z = 0)$ increases we observe in Fig. 3 are the result of preforming adsorbed layers created by solvent washing well-annealed films. In addition, the large $T_g(z = 0)$ increases only occur after long intermixing times suggesting that the pyrene-labeled chains are threading loops in the preformed adsorbed layer.

2. Group 2: Adsorbed Layers in the Limit of Zero Concentration

Figure 4 compares the temperature dependent fluorescence intensity curves used to measure $T_g(z = 0)$ for various different adsorbed layers from Group 2 with residual adsorbed layer thicknesses of only $h_{\text{ads}} \approx 1$ nm.

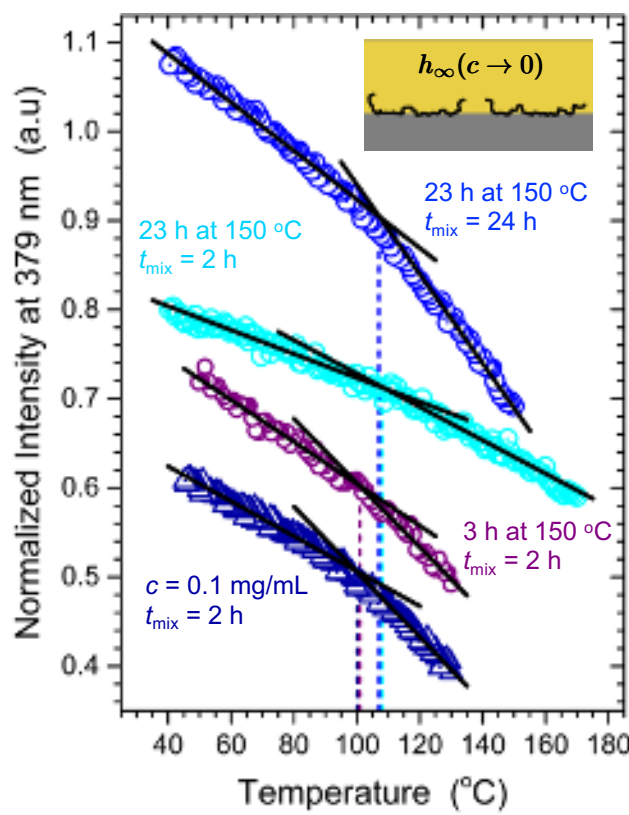


FIG. 4. Temperature-dependent fluorescence intensity data collected to measure the local $T_g(z = 0)$ next to substrates with different adsorbed layers from Group 2 in the limit of extremely low concentration $h_\infty(c \rightarrow 0)$ with $h_{ads} \approx 1$ nm. Solution grown adsorbed layer from $c = 0.1$ mg/mL (navy triangles), compared to films that were solvent washed for 100+ h after annealing for either 3 h (purple circles) or 23 h (cyan circles) at 150 °C with $t_{mix} = 2$ h, or 23 h annealed with $t_{mix} = 24$ h (blue circles).

Group 2 are adsorbed layers that result after a long time in solution in the limit of extremely low concentration $h_\infty(c \rightarrow 0)$, all with residual adsorbed layer thicknesses of $h_{ads} \approx 1$ nm. Specifically, we compare a solution grown adsorbed layer in the low concentration of $c = 0.1$ mg/mL, whose long-term plateau after 24+ h in solution resulted in $h_{ads} = 0.9$ nm. Recall that from Fig. 1, the same h_{ads} values are obtained after a sufficiently long time in solution for even lower concentrations like $c = 5 \times 10^{-3}$ mg/mL. The solvent-washed melt-annealed films are from annealing for either 3 h or 23 h at 150 °C and subsequently solvent washing for 100+ h in toluene to obtain residual adsorbed layer thicknesses of $h_{ads} = 1.1$ nm and 1.4 nm, respectively. Given the high mobility of adsorbed chains in solution,^{16–19} we believe these different adsorbed layers have been able to reach a roughly equivalent long-term state where chains are primarily extended on the surface forming long trains.⁴¹ For our high molecular weight chains in a good solvent, atomic force microscopy studies in the literature exam-

ining residual adsorbed layers after different solvent and annealing conditions suggest this is a near monolayer of surface coverage on the substrate interface with few small holes.^{67–69}

For all these adsorbed layers in the limit of extremely low concentration $h_\infty(c \rightarrow 0)$, we find the local $T_g(z = 0)$ value to be comparable to bulk T_g for PS. As shown in Fig. 4, $T_g(z = 0) = 100$ °C for the $c = 0.1$ mg/mL solution grown adsorbed layer with $h_{ads} = 0.9$ nm and $T_g(z = 0) = 101$ °C for the 3 h melt-annealed film washed 100+ h, where these used an intermixing time of $t_{mix} = 2$ h. Even the 23 h melt-annealed film washed 100+ h had a $T_g(z = 0)$ of only 108 °C for $t_{mix} = 2$ h and $T_g(z = 0) = 107$ °C after $t_{mix} = 24$ h, which is considerably reduced relative to the large $T_g(z = 0)$ increases observed in Fig. 3. The slight elevation in $T_g(z = 0)$ suggests that more time in solution is likely required to fully reequilibrate these adsorbed layers in solution and obtain $T_g(z = 0)$ values closer to T_g^{bulk} . The insensitivity of $T_g(z = 0)$ to the intermixing time t_{mix} at 170 °C for these very thin adsorbed layers with $h_{ads} \approx 1$ nm is unsurprising for such thin adsorbed layers that are primarily dominated by trains. This observation is consistent with work by Koga et al. showing that little to no adhesion is possible between a polymer matrix and such thin adsorbed layers, even under an applied load at high temperature.⁷⁰

C. Inferring the Structure of Adsorbed Chains and Understanding Their Impact on Local T_g

The adsorption and desorption process in solution has been well-studied in the literature.^{1,16} At higher solution concentrations, the surface crowding of chains leads to fewer surface contacts per chain (shorter trains) producing adsorbed chains with long tails and large fluffy loops. In contrast, at lower concentrations, each chain can spread out on the surface with long trains resulting in short tails and small loops. The adsorption lattice model developed by Scheutjens and Fleer can be used to get a sense of the tail, loop, and train distribution at different solution concentrations.^{41,42,48} This Scheutjens and Fleer model is a self-consistent mean field theory (SCFT) treatment formulated as a lattice theory similar to Flory-Huggins solution theory with an added interaction energy parameter χ_s to account for the substrate interaction. The substrate sticking energy is defined as

$$\chi_s = -(u_s - u_s^0)/k_B T, \quad (3)$$

the difference in free energy to transfer a polymer segment from bulk polymer to the substrate surface and the free energy to transfer a solvent molecule from pure solvent to the substrate surface.⁴⁸ A positive value of χ_s favors polymer contacts at the substrate interface.

Based on the Scheutjens and Fleer theory, the average tail length for a $c = 1$ mg/mL solution (volume fraction $\phi \simeq 10^{-3}$) is $\sim 10\%$ the total chain length,⁴² giving tails

of ~ 40 kg/mol for our $M_w = 400$ kg/mol; although this distribution of tail lengths is broad, especially at long tail lengths. Loop lengths are comparable to tail lengths, but as loops must return to the surface, they extend roughly half as far as tails from the surface.^{1,41} At very low concentrations, $c = 5 \times 10^{-3}$ mg/mL ($\phi \simeq 10^{-6}$), tail lengths are only $\sim 3\%$ the chain length,⁴² giving ~ 10 kg/mol for our $M_w = 400$ kg/mol, with loop lengths also being similarly short.^{1,41} Schematics of these tail, loop, and train distributions are illustrated in Fig. 1a.

Given these estimates of average tail and loop lengths from the Scheutjens and Fleer theory for adsorbed layers grown in solution,^{41,42} we revisit the differences in local $T_g(z = 0)$ with increasing intermixing time t_{mix} shown in Fig. 3c to inform us about what parts of the adsorbed layer impact the local T_g of the matrix. For the $c = 1$ mg/mL solution grown adsorbed layers with $h_{\text{ads}} = 5.2$ nm, the tails are expected to be ~ 40 kg/mol with comparably large fluffy loops.^{41,42} At long intermixing times $t_{\text{mix}} \geq 24$ h, the local $T_g(z = 0)$ is comparable to bulk T_g and the local T_g measured next to bare silica substrates with no adsorbed or grafted chains $T_g(z = 0) = 100 \pm 2$ °C. This suggests that intermixing with these ~ 40 kg/mol tails and threading of these comparably large fluffy loops by pyrene-labeled chains does not impart an increase in $T_g(z = 0)$. We suspect the slightly reduced $T_g(z = 0)$ observed at short intermixing times $t_{\text{mix}} = 2$ h likely results from trapped void space acting as free surface caused by the comparatively large fluffy loops of these solution grown adsorbed layers. It is worth noting that Burroughs et al. have also observed local T_g values less than T_g^{bulk} for capped adsorbed layers with minimal intermixing time.⁵² In fact, Ren et al. has shown that the degree of $T_g(h)$ increase that occurs in thin PS films due to the adsorbed layer correlates directly with the degree of overlap between the adsorbed chains and overlaying PS film as measured by neutron reflectivity.⁷¹

In contrast, chain adsorption in the melt is significantly less well understood. The problems with simply extending adsorption theories from solution to melts are two fold. The Eq. (3) definition of the substrate sticking energy χ_s used in solution becomes identically zero in polymer melts. Without the presence of solvent, there is no enthalpic reason to favor one polymer segment–surface contact over another because it is simply replaced with an equivalent polymer segment–surface contact. Thus, the free energy change associated with chain adsorption in melts is entirely entropic, determined by the statistics of chain conformations possible near the substrate interface.^{41,48,72} Assuming, of course, that the system is ergodic and in thermodynamic equilibrium.

However, more problematic with interpreting chain adsorption in the melt is that the kinetics are exceedingly slow, meaning the assumption of thermodynamic equilibrium made for adsorption theories in solution is likely not valid. The adsorbed layer formed in the melt will likely be more representative of some kinetically limited structure. To get an idea of what this may be, let us review what can

be concluded from the experimental observations of Figures 2 and 3. In Fig. 2, we found that melt annealed films took a much longer time in solution to reach the same limiting adsorbed layer amount $h_{\infty}^{\text{des}}(c \rightarrow 0)$ in the limit of zero concentration. This suggests that some evolution of the chains near the substrate interface has occurred to make their subsequent dynamics in solution slower. We posit that the chains remaining at the substrate interface have a larger number of polymer segment–surface contacts making them harder to displace in solution.

In Fig. 3, we investigated how the local $T_g(z = 0)$ varied with increasing intermixing time. For the short $t_{\text{mix}} = 2$ h that would allow for the interpenetration of tails, the local $T_g(z = 0)$ value is only slightly increased relative to T_g^{bulk} by a few degrees. From the $h_{\text{ads}} = 3.6$ nm for these melt-annealed films, we can calculate an effective density of tails $\sigma_{\text{tails}} = 2(\frac{\rho N_A h_{\text{ads}}}{M_n}) = 0.012$ tails/nm², assuming two tails per chain. This formula is based on that commonly used for determining grafting density from a measure of the dry brush thickness, where M_n is the number average molecular weight of the surface attached chains, N_A is Avogadro's number, and ρ the bulk density which for PS is 1.045 g/cm³.^{34,36,73} From our previous work measuring the local glass transition temperature of PS matrices next to end-grafted PS chains on silica, we would expect a $T_g(z = 0)$ increase of ≈ 45 K, independent of grafting density from 0.003 to 0.33 chain/nm² and grafted chain length between $M_n = 8.6$ kg/mol to 212 kg/mol.³⁶ Thus, it is clear that tails of adsorbed chains do not behave in the same manner to grafted chain ends when it comes to restricting the local mobility.

In contrast, at long intermixing times, the adsorbed layers from 30 min solvent washed films that were annealed at 150 °C for 23 h exhibited a significant increase in $T_g(z = 0)$ with increasing t_{mix} . After the intermixing time of $t_{\text{mix}} = 48$ h, the local $T_g(z = 0)$ is observed to increase by ≈ 30 K to $T_g(z = 0) = 131 \pm 2$ °C. As discussed in section III B 1, we have been able to rule out the possibility that this $T_g(z = 0)$ increase is caused by the desorption and exchange of chains during the intermixing time. Thus, we believe that the increase in $T_g(z = 0)$ with intermixing time associated with the 30 min solvent washed films is the threading of loops. Given the large ≈ 30 K $T_g(z = 0)$ increase, these loops must be more restrictive to the mobility of the pyrene-labeled PS chains than the large fluffy loops of the solution grown adsorbed layers, i.e., smaller than ~ 40 kg/mol. It is possible that the small increase in $T_g(z = 0)$ observed at $t_{\text{mix}} = 2$ h is caused by the initial threading of a few such small loops.

The melt annealing step is largely unknown, and what we seek to better understand. Given the conclusions we have been able to draw from the experimental results, let us consider how the chains near the substrate interface may evolve kinetically during melt annealing. The initial starting state of the polymer chains near the substrate surface in the freshly spin-coated film are likely not too far from that of an adsorbed layer formed in solution at relatively high concentration having long tails

and large loops.^{41,42} Sum frequency generation (SFG) spectroscopy measurements by Dhinojawala and coworkers have found that the local monomer orientation at the substrate interface for poly(methyl methacrylate) (PMMA) spin-coated films is similar to that observed for adsorbed layers formed in solution.⁷⁴ Next, consider the process of monomer and chain exchange at a substrate surface. In solution, individual polymer segment–surface contacts continuously detach and reattach, over time exchanging with solvent or other polymer segment–surface contacts from another chain.²¹ In this manner, a given adsorbed chain can unzip from the surface and drift away. The rate limiting step in this desorption process is often considered to be the final diffusion of the desorbed chain away from the surface.²⁰ If we consider this process in a melt, the exchange of polymer segment–surface contacts should occur readily at the surface interface at a rate associated with local segmental dynamics. However, the final diffusion away from the interface, especially for entangled polymer melts, will be exceedingly slow. Over prolonged annealing in the melt, we can expect that chains with initially few segment–surface contacts will be the ones more likely able to drift away. These surface contacts will be replaced with contacts from neighboring polymer chains that are more likely to already have many segment–surface contacts. In this manner, we suspect that this kinetic process leads to a coarsening of the number of polymer segment–surface contacts per chain, favoring those chains with already the greatest number of contacts with the surface. In **Figure 5a**, we illustrate this proposed coarsening mechanism of polymer segment–surface contacts. Consistent with our experimental observations, such a mechanism would result in a layer of chains near the substrate interface with a larger number of polymer segment–surface contacts per chain making their subsequent kinetics in solution slower, and would lead to a shrinking of loop sizes as the neighboring trains increase in length.

In **Figure 5b**, we summarize our findings by illustrating the various different mechanisms we have identified that can cause local T_g changes to PS matrices at PS/silica interfaces. The adsorbed layers grown in solution with $c = 1.0$ mg/mL have comparatively large loops and tails of ~ 40 kg/mol for our 400 kg/mol M_w .^{41,42} These adsorbed layers did not cause any increase in $T_g(z = 0)$, even at long intermixing times indicating such large loops and tails do not provide any restriction in local mobility. At small intermixing times a slight T_g reduction below T_g^{bulk} was observed for these fluffy adsorbed layers indicating some trapped free surface. In contrast, adsorbed layers resulting from 30-min solvent washing of well melt-annealed films at 150 °C for 23 h produced a large +30 K increase in $T_g(z = 0)$ at long intermixing times that we attribute to the threading of small loops. Unsurprisingly, the thin $h_{\text{ads}} \approx 1$ nm adsorbed layers with predominantly trains obtained after a long time in solution in the limit of low concentration $h_{\infty}(c \rightarrow 0)$ did not result in $T_g(z = 0)$ increases, regardless of intermix-

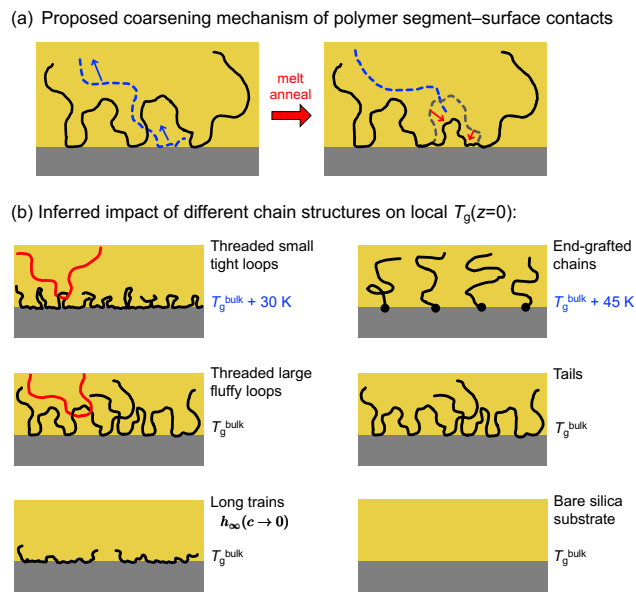


FIG. 5. (a) Schematic illustration of the proposed coarsening process occurring during melt annealing that increases the number of polymer segment–surface contacts per chain for those chains with already many segment–surface contacts, thereby increasing the length of their trains and decreasing the size of loops. (b) Illustration of the various different factors we have identified that cause local $T_g(z = 0)$ increases of matrix PS chains next to silica substrates, along with the many that do not. From the present work, we conclude that adsorbed layers are only able to cause large increases in the local $T_g(z = 0)$ when PS matrix chains are able to thread small loops resulting in $T_g(z = 0) + 30$ K. In contrast, larger loops, trains, and tails do not impact $T_g(z = 0)$. The latter is surprising given our previous work showing that end-grafted PS chains cause large +45 K increases in $T_g(z = 0)$ independent of grafting density and chain length,³⁶ suggesting that chemical grafting is distinctly different from physically adsorbed segments. These changes in $T_g(z = 0)$ are all topological in origin as the bare PS/silica interface does not perturb $T_g(z = 0)$, even after 48 h of annealing at 170 °C.

ing time. We find that tails have essentially no impact on local T_g compared with end-grafted chains. Recent results from our group found that end-grafted PS-OH or PS-COOH chains with $M_n = 8.6$ kg/mol to 212 kg/mol result in large $T_g(z = 0)$ increases of +45 K independent of grafting density.³⁶ This suggests that adsorbed tails do not provide the same immobilization as the covalent bond of grafts.

What sized loops cause increases in local T_g ? Based on the theory of Scheutjens and Fleer,^{41,42} the $c = 1.0$ mg/mL solution grown adsorbed layers have loop sizes ~ 40 kg/mol. As these adsorbed layers do not cause any increase in the measured $T_g(z = 0)$ value, we conclude that such large fluffy loops do not provide any significant restriction in mobility. In contrast, the 30 min solvent washed films that were annealed at 150 °C for 23 h exhibited a large increase in $T_g(z = 0)$. How-

ever, it is unclear what sized loops such adsorbed layers may have other than we anticipate that melt annealing leads to a decrease in loop size. It is interesting to compare to the film average glass transition temperature $T_g(h)$ measurements by Zuo et al. on poly(styrene-*r*-4-hydroxystyrene) P(S-*r*-HS) copolymer where the random hydroxystyrene monomers act as strong pinning sites causing loops.⁷⁵ Notable increases in $T_g(h)$ relative to the behavior of $T_g(h)$ for regular PS films were observed for the largest loops they measured that were only ~ 4.5 kg/mol in size, which we suspect were the easiest to thread. A systematic study of $T_g(z = 0)$ for different loop sizes would be warranted.

It is worth noting that the average density of loops per chain is relatively large for high molecular weight polymers with upwards of $\sim 60\%$ of the chain segments in loops for 1 mg/mL solution grown adsorbed layers.^{1,41} For loop lengths comparable to tail lengths,^{41,42} this would give us an average of approximately 5 loops per chain for our 400 kg/mol PS chains, resulting in an average loop density of order 0.05 loops/nm² for the solution grown adsorbed layers at $c = 1$ mg/mL. For the solvent washed films, again much is unknown. However, the average surface density of loops for the initially spin-coated films were probably not much different than that for solution grown adsorbed layers at high concentration. The subsequent annealing of the film in the melt state would then be expected to shrink these loops to a smaller size as the length of the trains increase for the most well adhered chains. In both cases, it is clear the surface is covered with many more loops than tails.

IV. CONCLUSIONS

We have compared the well understood system of adsorbed layers grown in solution to the solvent washing characteristics of adsorbed layers formed by annealing bulk polymer films in the melt state for extended periods of time. In the limit of zero concentration, we find that the same limiting adsorbed amount $h_{\infty}^{\text{ads}}(c \rightarrow 0) \approx 1$ nm is reached at long times strongly suggesting there is a thermodynamic equilibrium state likely corresponding to a near monolayer of surface coverage with few chains remaining in the bulk solution. On desorption, this same limiting adsorbed amount $h_{\infty}^{\text{des}}(c \rightarrow 0) \approx 1$ nm is reached at long times by both adsorbed layers formed in solution and from solvent washing melt annealed films. As both systems are now equivalent, adsorbed layers in solution, the same physics must apply. Longer annealing times in the melt state slow the dynamics of this desorption process, which we attribute to the chains near the substrate interface having more polymer segment–surface contacts per chain.

By leveraging the wealth of existing understanding about polymer conformations in solution, we are able to deduce distinctions in chain conformations between the different kinds of adsorbed layers. For the well-

understood system of solution grown adsorbed layers, the theory of Scheutjens and Fleer can provide a reasonable estimate of the length of loops, tails, and trains at different solution concentrations c .^{41,42} In contrast, the impact of melt annealing on the conformations of chains near the substrate interface is comparatively unknown. When no solvent is present in the melt, there is no enthalpic driving force for adsorption as the difference between one polymer segment–surface contact and another are equivalent. We propose that extended annealing in the melt state causes a coarsening of the number of polymer segment–surface contacts that favors chains with the most number of existing polymer segment–surface contacts, increasing the length of their trains and shrinking loops and tails.

A multilayer sample geometry was utilized to measure the local glass transition temperature $T_g(z = 0)$ with pyrene fluorescence of PS matrix chains intermixed with the different types of adsorbed layers formed on silica substrates. The total thickness of the multilayer film is large enough to avoid competing interfacial perturbations from the free surface, isolating the impact the adsorbed chains can have. The PS/silica system we are working with is athermal in that the bare silica substrate does not impact the local $T_g(z = 0)$ of the pyrene-labeled PS chains, even when annealed for 48 h at 170 °C, meaning the observed $T_g(z = 0)$ changes are entirely topological in origin. In particular, we compare two different groups of adsorbed layers. The first having relatively thick adsorbed layers with residual adsorbed layer thicknesses $h_{\text{ads}} \approx 4.5$ nm, while the second with $h_{\text{ads}} \approx 1$ nm are in the limit of low concentration $h_{\infty}(c \rightarrow 0)$ after the adsorbed layers have spent a long time in solution. In each group, we compare the well-understood system of solution grown adsorbed layers with the comparatively unknown system of adsorbed layers obtained after solvent washing films that were annealed in the melt state. By varying the time scale t_{mix} for intermixing the pyrene-labeled PS matrix chains with the adsorbed layer, we are able to discriminate between the impact loops, tails, and trains can have on the local T_g of matrix chains. At short intermixing times of $t_{\text{mix}} = 2$ h, tails are able to intermix with the pyrene-labeled PS chains, while longer intermixing times, up to $t_{\text{mix}} = 48$ h, would allow for the threading of loops. In contrast, to our previous work on end-grafted chains,^{34,36} we find that tails do not impart any local T_g increase. The only local T_g increase we observe from adsorbed layers is a ≈ 30 K increase in $T_g(z = 0)$ above bulk T_g for adsorbed layers formed by 30-min of solvent washing films that were melt annealed at 150 °C for 23 h, which we attribute to the threading of small tight loops.

ACKNOWLEDGMENTS

Funding from the National Science Foundation Polymers Program (DMR-1709132 and DMR-1905782) and Emory University is gratefully acknowledged.

AUTHOR DECLARATIONS

Conflict of interest

The authors have no conflicts to disclose.

DATA AVAILABILITY

The data that supports the findings of this study are available within the article, and further raw data files are available from the corresponding author upon reasonable request.

REFERENCES

- ¹G. J. Fleer, M. A. Cohen Stuart, J. M. H. M. Scheutjens, T. Cosgrove, and B. Vincent, *Polymers at Interfaces* (Chapman & Hall, London, UK, 1993).
- ²R. A. L. Jones and R. W. Richards, *Polymers at Surfaces and Interfaces* (Cambridge University Press, Cambridge, UK, 1999).
- ³L. Léger and C. Creton, "Adhesion mechanisms at soft polymer interfaces," *Philosophical Transactions of the Royal Society A: Mathematical, Physical and Engineering Sciences* **366**, 1425–1442 (2008).
- ⁴S. K. Kumar, B. C. Benicewicz, R. A. Vaia, and K. I. Winey, "50th Anniversary Perspective: Are Polymer Nanocomposites Practical for Applications?" *Macromolecules* **50**, 714–731 (2017).
- ⁵E. J. Bailey and K. I. Winey, "Dynamics of polymer segments, polymer chains, and nanoparticles in polymer nanocomposite melts: A review," *Progress in Polymer Science* **105**, 101242 (2020).
- ⁶D. Salatto, J.-M. Y. Carrillo, M. K. Endoh, T. Taniguchi, B. M. Yavitt, T. Masui, H. Kishimoto, M. Tyagi, A. E. Ribbe, V. G. Sakai, M. Kruteva, B. G. Sumpter, B. Farago, D. Richter, M. Nagao, and T. Koga, "Structural and Dynamical Roles of Bound Polymer Chains in Rubber Reinforcement," *Macromolecules* **54**, 11032–11046 (2021).
- ⁷E. Senses, A. Isherwood, and P. Akcora, "Reversible Thermal Stiffening in Polymer Nanocomposites," *ACS Applied Materials & Interfaces* **7**, 14682–14689 (2015).
- ⁸E. Senses, A. Faraone, and P. Akcora, "Microscopic Chain Motion in Polymer Nanocomposites with Dynamically Asymmetric Interphases," *Scientific Reports* **6**, 29326 (2016).
- ⁹M. F. Thees, J. A. McGuire, and C. B. Roth, "Review and reproducibility of forming adsorbed layers from solvent washing of melt annealed films," *Soft Matter* **16**, 5366–5387 (2020).
- ¹⁰N. Jouault, J. F. Moll, D. Meng, K. Windsor, S. Ramcharan, C. Kearney, and S. K. Kumar, "Bound Polymer Layer in Nanocomposites," *ACS Macro Letters* **2**, 371–374 (2013).
- ¹¹A. M. Jimenez, D. Zhao, K. Misquitta, J. Jestin, and S. K. Kumar, "Exchange Lifetimes of the Bound Polymer Layer on Silica Nanoparticles," *ACS Macro Letters* **8**, 166 – 171 (2019).
- ¹²E. Y. Lin, A. L. Frischknecht, K. I. Winey, and R. A. Riggleman, "Effect of surface properties and polymer chain length on polymer adsorption in solution," *Journal of Chemical Physics* **155**, 034701 (2021).
- ¹³C. J. Durning, B. O'Shaughness, U. Sawhney, D. Nguyen, J. Majewski, and G. S. Smith, "Adsorption of Poly(methyl methacrylate) Melts on Quartz," *Macromolecules* **32**, 6772–6781 (1999).
- ¹⁴S. Napolitano, "Irreversible adsorption of polymer melts and nanoconfinement effects," *Soft Matter* **16**, 5348–5365 (2020).
- ¹⁵E. Jenckel and B. Rumbach, "Über die Adsorption von hochmolekularen Stoffen aus der Lösung," *Zeitschrift für Elektrochemie und angewandte physikalische Chemie* **55**, 612 – 618 (1951).
- ¹⁶S. Granick, "Chap. 10: Dynamics of Adsorption and Desorption at Polymer/Solid Interfaces," in *Physics of Polymer Surfaces and Interfaces*, edited by I. C. Sanchez (Butterworth-Heinemann, Boston, 1992) pp. 227–244.
- ¹⁷C. Yu and S. Granick, "Revisiting Polymer Surface Diffusion in the Extreme Case of Strong Adsorption," *Langmuir* **30**, 14538–14544 (2014).
- ¹⁸C. Yu, J. Guan, K. Chen, S. C. Bae, and S. Granick, "Single-Molecule Observation of Long Jumps in Polymer Adsorption," *ACS Nano* **7**, 9735–9742 (2013).
- ¹⁹J. Zhao and S. Granick, "How Polymer Surface Diffusion Depends on Surface Coverage," *Macromolecules* **40**, 1243–1247 (2007).
- ²⁰J. F. Douglas, H. E. Johnson, and S. Granick, "A Simple Kinetic Model of Polymer Adsorption and Desorption," *Science* **262**, 2010–2012 (1993).
- ²¹P. G. de Gennes, "Polymers at an interface; a simplified view," *Advances in Colloid and Interface Science* **27**, 189–209 (1987).
- ²²S. Chandran, J. Baschnagel, D. Cangialosi, K. Fukao, E. Glynnos, L. M. C. Janssen, M. Muller, M. Muthukumar, U. Steiner, J. Xu, S. Napolitano, and G. Reiter, "Processing Pathways Decide Polymer Properties at the Molecular Level," *Macromolecules* **52**, 7146–7156 (2019).
- ²³Y. Fujii, Z. Yang, J. Leach, H. Atarashi, K. Tanaka, and O. K. C. Tsui, "Affinity of Polystyrene Films to Hydrogen-Passivated Silicon and Its Relevance to the Tg of the Films," *Macromolecules* **42**, 7418–7422 (2009).
- ²⁴O. Guiselin, "Irreversible Adsorption of a Concentrated Polymer Solution," *Europhysics Letters* **17**, 225–230 (1992).
- ²⁵P. Gin, N. Jiang, C. Liang, T. Taniguchi, B. Akgun, S. K. Satija, M. K. Endoh, and T. Koga, "Revealed Architectures of Adsorbed Polymer Chains at Solid-Polymer Melt Interfaces," *Physical Review Letters* **109**, 265501 (2012).
- ²⁶N. Jiang, J. Shang, X. Di, M. K. Endoh, and T. Koga, "Formation Mechanism of High-Density, Flattened Polymer Nanolayers Adsorbed on Planar Solids," *Macromolecules* **47**, 2682–2689 (2014).
- ²⁷M. Sen, N. Jiang, J. Cheung, M. K. Endoh, T. Koga, D. Kawaguchi, and K. Tanaka, "Flattening Process of Polymer Chains Irreversibly Adsorbed on a Solid," *ACS Macro Letters* **5**, 504–508 (2016).
- ²⁸C. Housmans, M. Sferrazza, and S. Napolitano, "Kinetics of Irreversible Chain Adsorption," *Macromolecules* **47**, 3390–3393 (2014).
- ²⁹D. Nieto Simavilla, A. Panagopoulou, and S. Napolitano, "Characterization of Adsorbed Polymer Layers: Preparation, Determination of the Adsorbed Amount and Investigation of the Kinetics of Irreversible Adsorption," *Macromolecular Chemistry and Physics* **219**, 1700303 (2018).
- ³⁰D. Nieto Simavilla, W. Huang, P. Vandestrick, J.-P. Ryckaert, M. Sferrazza, and S. Napolitano, "Mechanisms of Polymer Adsorption onto Solid Substrates," *ACS Macro Letters* **6**, 975–979 (2017).
- ³¹D. Nieto Simavilla, W. Huang, C. Housmans, M. Sferrazza, and S. Napolitano, "Taming the Strength of Interfacial Interactions via Nanoconfinement," *ACS Central Science* **4**, 755–759 (2018).
- ³²M. Gawek, H. Omar, P. Szymoniak, and A. Schönhals, "Growth kinetics of the adsorbed layer of poly(2-vinylpyridine) – an indirect observation of desorption of polymers from substrates," *Soft Matter* **19**, 3975–3982 (2023).
- ³³C. J. Ellison and J. M. Torkelson, "The distribution of glass-transition temperatures in nanoscopically confined glass formers," *Nature Materials* **2**, 695 – 700 (2003).
- ³⁴X. Huang and C. B. Roth, "Optimizing the Grafting Density of Tethered Chains to Alter the Local Glass Transition Temperature of Polystyrene near Silica Substrates: The Advantage of Mushrooms over Brushes," *ACS Macro Letters* **7**, 269–274 (2018).
- ³⁵X. Huang, M. F. Thees, W. B. Size, and C. B. Roth, "Experimental study of substrate roughness on the local glass transition of polystyrene," *Journal of Chemical Physics* **152**, 244901 (2020).
- ³⁶J. H. Merrill, R. Li, and C. B. Roth, "End-Tethered Chains Increase the Local Glass Transition Temperature of Matrix Chains by 45 K Next to Solid Substrates Independent of Chain Length," *ACS Macro Letters* **12**, 1–7 (2023).
- ³⁷X. Huang and C. B. Roth, "Changes in the temperature-

dependent specific volume of supported polystyrene films with film thickness," *Journal of Chemical Physics* **144**, 234903 (2016).

³⁸H. Fujiwara, *Spectroscopic Ellipsometry: Principles and Applications* (John Wiley & Sons, West Sussex, England, 2007).

³⁹H. G. Tompkins, *A User's Guide to Ellipsometry* (Academic Press, San Diego, CA, 1993).

⁴⁰P. M. Rauscher, J. E. Pye, R. R. Baglay, and C. B. Roth, "Effect of Adjacent Rubbery Layers on the Physical Aging of Glassy Polymers," *Macromolecules* **46**, 9806–9817 (2013).

⁴¹J. M. H. M. Scheutjens and G. J. Fleer, "Statistical theory of the adsorption of interacting chain molecules. 2. Train, loop, and tail size distribution," *Journal of Physical Chemistry* **84**, 178–190 (1980).

⁴²J. M. H. M. Scheutjens, G. J. Fleer, and M. A. Cohen Stuart, "End Effects in Polymer Adsorption: A Tale of Tails," *Colloids and Surfaces* **21**, 285–306 (1986).

⁴³G. P. van der Beek, M. A. Cohen Stuart, G. J. Fleer, and J. E. Hofman, "A chromatographic method for the determination of segmental adsorption energies of polymers. Polystyrene on silica," *Langmuir* **5**, 1180–1186 (1989).

⁴⁴G. Kraus and J. Dugone, "Adsorption of Elastomers on Carbon Black," *Industrial & Engineering Chemistry* **47**, 1809–1816 (1955).

⁴⁵W. H. Grant, L. E. Smith, and R. R. Stromberg, "Adsorption and Desorption Rates of Polystyrene on Flat Surfaces," *Faraday Discussions of the Chemical Society* **59**, 209–217 (1975).

⁴⁶P. Frantz and S. Granick, "Kinetics of polymer adsorption and desorption," *Physical Review Letters* **66**, 899–902 (1991).

⁴⁷H. M. Schneider and S. Granick, "Kinetic traps in polymer adsorption: exchange of polystyrene between the adsorbed state and a good solvent," *Macromolecules* **25**, 5054–5059 (1992).

⁴⁸J. M. H. M. Scheutjens and G. J. Fleer, "Statistical theory of the adsorption of interacting chain molecules. 1. Partition function, segment density distribution, and adsorption isotherms," *Journal of Physical Chemistry* **83**, 1619–1635 (1979).

⁴⁹E. Pefferkorn, A. Carroy, and R. Varoqui, "Dynamic behavior of flexible polymers at a solid/liquid interface," *Journal of Polymer Science: Polymer Physics Edition* **23**, 1997–2008 (1985).

⁵⁰R. R. Baglay and C. B. Roth, "Communication: Experimentally determined profile of local glass transition temperature across a glassy-rubbery polymer interface with a T_g difference of 80 K," *Journal of Chemical Physics* **143**, 111101 (2015).

⁵¹R. R. Baglay and C. B. Roth, "Local glass transition temperature T_{g(z)} of polystyrene next to different polymers: Hard vs. soft confinement," *Journal of Chemical Physics* **146**, 203307 (2017).

⁵²M. J. Burroughs, S. Napolitano, D. Cangialosi, and R. D. Priestley, "Direct Measurement of Glass Transition Temperature in Exposed and Buried Adsorbed Polymer Nanolayers," *Macromolecules* **49**, 4647–4655 (2016).

⁵³K. Randazzo, M. Bartkiewicz, B. Graczykowski, D. Cangialosi, G. Fytas, B. Zuo, and R. D. Priestley, "Direct Visualization and Characterization of Interfacially Adsorbed Polymer atop Nanoparticles and within Nanocomposites," *Macromolecules* **54**, 10224–10234 (2021).

⁵⁴T. Wei and J. M. Torkelson, "Molecular Weight Dependence of the Glass Transition Temperature (T_g)-Confinement Effect in Well-Dispersed Poly(2-vinyl pyridine)-Silica Nanocomposites: Comparison of Interfacial Layer T_g and Matrix T_g," *Macromolecules* **53**, 8725–8736 (2020).

⁵⁵Z. Jiang, B. Cheng, J. Yang, and J. Zhao, "Free Space Makes the Polymer "Dead Layer" Alive," *Journal of Physical Chemistry B* **126**, 10750–10757 (2022).

⁵⁶B. Valeur and M. N. Berberan-Santos, *Molecular Fluorescence: Principles and Applications* (Wiley-VCH, Weinheim, Germany, 2012).

⁵⁷K. Kalyanasundaram and J. K. Thomas, "Environmental Effects on Vibronic Band Intensities in Pyrene Monomer Fluorescence and Their Application in Studies of Micellar Systems," *Journal of the American Chemical Society* **99**, 2039 – 2044 (1977).

⁵⁸C. B. Roth, "Polymers under nanoconfinement: Where are we now in understanding local property changes?" *Chemical Society Reviews* **50**, 8050–8066 (2021).

⁵⁹C. J. Clarke, "The kinetics of polymer brush penetration in to a high molecular weight matrix," *Polymer* **37**, 4747–4752 (1996).

⁶⁰M. Geoghegan, C. J. Clarke, F. Boué, A. Menelle, T. Russ, and D. G. Bucknall, "The Kinetics of Penetration of Grafted Polymers into a Network," *Macromolecules* **32**, 5106–5114 (1999).

⁶¹A. Chennevière, E. Drockenmuller, D. Damiron, F. Cousin, F. Boué, F. Restagno, and L. Léger, "Quantitative Analysis of Interdigitation Kinetics between a Polymer Melt and a Polymer Brush," *Macromolecules* **46**, 6955–6962 (2013).

⁶²K. P. O'Connor and T. C. B. McLeish, "Molecular velcro": dynamics of a constrained chain into an elastomer network," *Macromolecules* **26**, 7322–7325 (1993).

⁶³K. O'Connor and T. McLeish, "Entangled dynamics of healing end-grafted chains at a solid/polymer interface," *Faraday Discussions* **98**, 67–78 (1994).

⁶⁴S. Granick, "Perspective: Kinetic and mechanical properties of adsorbed polymer layers," *European Physical Journal E* **9**, 421–424 (2002).

⁶⁵E. J. Bailey, P. J. Griffin, R. J. Composto, and K. I. Winey, "Characterizing the Areal Density and Desorption Kinetics of Physically Adsorbed Polymer in Polymer Nanocomposite Melts," *Macromolecules* **53**, 2744–2753 (2020).

⁶⁶W. Ren, Y. Li, Y. Tang, J. Xu, C. Zhang, O. K. C. Tsui, and X. Wang, "Loosely Adsorbed Chains Expedite the Desorption of Flattened Polystyrene Chains on Flat Silicon Surface," *ACS Macro Letters* **12**, 854–859 (2023).

⁶⁷N. Jiang, J. M. Cheung, Y. Guo, M. K. Endoh, T. Koga, G. Yuan, and S. K. Satija, "Stability of Adsorbed Polystyrene Nanolayers on Silicon Substrates," *Macromolecular Chemistry and Physics* **219**, 1700326 (2018).

⁶⁸A. Beena Unni, G. Vignaud, J. K. Bal, N. Delorme, T. Beuvier, S. Thomas, Y. Grohens, and A. Gibaud, "Solvent Assisted Rinsing: Stability/Instability of Ultrathin Polymer Residual Layer," *Macromolecules* **49**, 1807–1815 (2016).

⁶⁹W. Xu, K. Mihhels, N. Kotov, S. Lepikko, R. H. Ras, C. M. Johnson, T. Pettersson, and E. Kontturi, "Solid-state polymer adsorption for surface modification: The role of molecular weight," *Journal of Colloid and Interface Science* **605**, 441–450 (2022).

⁷⁰N. Jiang, M. Sen, W. Zeng, Z. Chen, J. M. Cheung, Y. Morimitsu, M. K. Endoh, T. Koga, M. Fukuto, G. Yuan, S. K. Satija, J.-M. Y. Carrillo, and B. G. Sumpter, "Structure-induced switching of interpolymer adhesion at a solid–polymer melt interface," *Soft Matter* **14**, 1108–1119 (2018).

⁷¹W. Ren, X. Wang, J. Shi, J. Xu, H. Taneda, N. L. Yamada, D. Kawaguchi, K. Tanaka, and X. Wang, "The role of the molecular weight of the adsorbed layer on a substrate in the suppressed dynamics of supported thin polystyrene films," *Soft Matter* **18**, 1997–2005 (2022).

⁷²J. M. H. M. Scheutjens, "Chap. 6: Mean-Field Lattice Models of Polymers at Interfaces," in *Physics of Polymer Surfaces and Interfaces*, edited by I. C. Sanchez (Butterworth-Heinemann, Boston, 1992) pp. 117–138.

⁷³W. J. Brittain and S. Minko, "A structural definition of polymer brushes," *Journal of Polymer Science Part A: Polymer Chemistry* **45**, 3505–3512 (2007).

⁷⁴A. Rao, H. Rangwala, V. Varshney, and A. Dhinojwala, "Structure of Poly(methyl methacrylate) Chains Adsorbed on Sapphire Probed Using Infrared-Visible Sum Frequency Generation Spectroscopy," *Langmuir* **20**, 7183–7188 (2004).

⁷⁵B. Zuo, H. Zhou, M. J. B. Davis, X. Wang, and R. D. Priestley, "Effect of Local Chain Conformation in Adsorbed Nanolayers on Confined Polymer Molecular Mobility," *Physical Review Letters* **122**, 217801 (2019).